

# Magnon Dispersion and Anisotropies in $\text{SrCu}_2(\text{BO}_3)_2$

Y. F. Cheng<sup>1</sup>, O. Cepas<sup>2</sup>, P. W. Leung<sup>1</sup>, and T. Ziman<sup>3</sup>

<sup>1</sup>: Department of Physics, Hong Kong University of Science and Technology, Clear Water Bay, Hong Kong.

<sup>2</sup>: Laboratoire de physique theorique de la matiere condensee,  
UMR 7600 C.N.R.S., Universite Pierre et Marie Curie, Paris, France.

<sup>3</sup>: Institut Laue Langevin, BP 156, F-38042 Grenoble Cedex 9, France.

(dated: March 23, 2024)

We study the dispersion of the magnons (triplet states) in  $\text{SrCu}_2(\text{BO}_3)_2$  including all symmetry-allowed Dzyaloshinskii-Moriya interactions. We can reduce the complexity of the general Hamiltonian to a simpler form by appropriate rotations of the spin operators. The resulting Hamiltonian is studied by both perturbation theory and exact numerical diagonalization on a 32-site cluster. We argue that the dispersion is dominated by Dzyaloshinskii-Moriya interactions. We point out which combinations of these anisotropies affect the dispersion to linear-order, and extract their magnitudes.

## I. INTRODUCTION

Strontium copperboron oxide ( $\text{SrCu}_2(\text{BO}_3)_2$ ) is a two-dimensional antiferromagnet with no long-range magnetic order.<sup>1,2</sup> Heisenberg interactions between the  $S = 1/2$  magnetic moments are strong and the geometry is such that the planes of spin dimers are coupled in a way equivalent to those of the Shastry-Sutherland model.<sup>3,4</sup> This model had been proposed on purely theoretical grounds, and is remarkable in that while strongly interacting, it has an exact dimer ground state, fully isotropic in spin-space, up to a critical value of the coupling.<sup>3</sup> It is not integrable, however, and neither the excited states, nor their dispersions are known exactly. This motivated many studies of the dynamics of this model. The existence of a compound which is well modeled by the Shastry-Sutherland Hamiltonian, and what is more, is in an intermediate range of coupling, not far from a quantum critical point, is then of great interest. The spin excitations of  $\text{SrCu}_2(\text{BO}_3)_2$  have been studied extensively by a variety of experimental techniques (see e.g. [5,6] and references below). An immediate question is how to extract the couplings and to give a precise answer to the question: to what extent  $\text{SrCu}_2(\text{BO}_3)_2$  can be described by the Shastry-Sutherland model?

The first observation is that while the Shastry-Sutherland model and its ground state are rotationally invariant,  $\text{SrCu}_2(\text{BO}_3)_2$  shows departures from spin isotropy. Electron spin resonance (ESR),<sup>7</sup> far-infrared spectroscopy of forbidden transitions,<sup>8</sup> neutron inelastic scattering,<sup>9</sup> or latter Raman scattering<sup>10</sup> have shown the splitting of the spin triplet excitations at  $q = 0$  and anisotropic behavior with respect to the direction of an external magnetic field. This was explained<sup>9</sup> as originating from a Dzyaloshinskii-Moriya interaction (a correction of spin-orbit origin)<sup>11</sup> whose characteristic vector is oriented perpendicular to the copper planes, along the  $c$ -direction of the crystal. While spin-orbit interactions always introduce anisotropies at some energy scale, it was a surprise that in a frustrated model they could dominate the dispersion which generally arises from larger, isotropic, couplings. More recently, other components of the vectors were argued to be required to explain further

experimental findings: another splitting was observed at  $q = (\pi, 0)$ ,<sup>12,13</sup> and was subsequently associated with in-plane components of the Dzyaloshinskii-Moriya interactions. In addition, there is an avoided level crossing when the first triplet state is about to cross the ground state for magnetic fields applied along  $c$ . This is not compatible with a single-axis anisotropy along the same direction, and requires additional forms of anisotropy. The level anti-crossing was argued to be due to the nearest neighbor Dzyaloshinskii-Moriya interaction,<sup>14,15,16</sup> which was considered as a possible explanation for the X-band ESR as well.<sup>17</sup> All these components are indeed allowed by the symmetry of the crystal structure in the low temperature phase of  $\text{SrCu}_2(\text{BO}_3)_2$ ,<sup>18,19,20</sup> whose copper planes are slightly buckled. Were it not buckled (as in the high temperature phase<sup>19</sup>), these components would have vanished. It was for this reason that they were neglected in the original interpretation of the neutron inelastic scattering.<sup>9</sup> Nonetheless, because the symmetry is slightly broken these interactions are expected to be present and define a smaller energy scale.

A precise model for  $\text{SrCu}_2(\text{BO}_3)_2$  must therefore include, in addition to the larger Heisenberg couplings, a complex pattern of Dzyaloshinskii-Moriya interactions. Since their relative strengths are not precisely known, it is difficult to establish a hierarchy among them, other than the probable dominance of the  $c$ -axis component.

In this paper, we argue, on the basis of exact transformations and numerical diagonalizations, that we can simplify the model and determine the parameters of the transformed model by studying the dispersion of the triplet states. The dispersion of the triplet states of the Shastry-Sutherland model, taken alone, is very small, and this is why smaller interactions are relevant, and even turn out to be dominant.<sup>9</sup> It is natural to consider Dzyaloshinskii-Moriya interactions since they are linear in the ratio of the spin-orbit coupling to the crystal-field splitting,  $\Delta$ , which is estimated from the  $g$ -factor, i.e.  $\frac{g-2}{2}$  to be about 0.1. They are, however, peculiar, in that they are usually expected to have little effect on the spectrum, at most <sup>2,21</sup> It has even been claimed that Dzyaloshinskii-Moriya interactions and second-order symmetric anisotropic couplings

conspire to restore the rotational invariance of the spin excitation spectrum.<sup>21</sup> While this can be true for single-band models in certain geometries, here the frustration of the lattice makes such arguments inapplicable, as we shall see. We can in fact classify the Dzyaloshinskii-Moriya components into reducible components (that can be reduced to  $^2$  effects) and irreducible components that have effects on the dispersion linear in the spin-orbit coupling. The latter thus defines a larger energy scale which will be the focus of our discussion.

The problem then is to calculate the spin excitation spectrum reliably. If only isotropic interactions are considered,  $\text{SrCu}_2(\text{BO}_3)_2$  is very close in parameter space ( $J^0=J=0.62$ ) to a quantum critical point,<sup>4</sup> ( $J^0=J=0.68$ ), which separates the dimer phase (which is known exactly) to a phase that is not known exactly but may be quadrumerized.<sup>22,23,24</sup> Perturbative approaches to the excitations may therefore turn out to be inaccurate. For instance, the splitting of the  $q=0$  triplet energy is given by  $\Delta = D^0_2 g(J^0=J)$ , which is linear in  $D^0_2$  and involves a function  $g(J^0=J)$  with  $g(0)=4$ , but  $g(J^0=J)=2.0$  for  $J^0=J=0.62$ .<sup>9</sup> This is difficult to calculate by perturbative techniques because of the proximity with the quantum critical point. Therefore, in order to explain the dispersion of the first triplet states in  $\text{SrCu}_2(\text{BO}_3)_2$ , we need not only to include the relevant Dzyaloshinskii-Moriya interactions, but also to go beyond the perturbative techniques used earlier for the dispersion.<sup>4,25,26</sup> Indeed, even carried at high order in perturbation theory, such calculations may tend to overestimate the dispersion, as we shall see. For these reasons, we have carried out an exact numerical study of the model, including the Dzyaloshinskii-Moriya interactions.

In addition to symmetry-allowed components of the Dzyaloshinskii-Moriya vectors, other components, that are not allowed by the measured crystal symmetry were invoked<sup>27,28</sup> as possible explanations for the specific heat and the ESR "forbidden" transition. We shall not consider them here because, on one hand, no distortions of the crystal structure that would allow them have been reported so far,<sup>19,20</sup> and electric-dipole transitions provide a symmetry-preserving alternative to explain forbidden transitions.<sup>9,29</sup> Although it is not clear whether ESR are of magnetic-dipole or electric-dipole nature, it has been shown that the forbidden transitions observed by far infrared spectroscopy were clearly electric-dipole.<sup>30</sup> Even if the ESR transitions were magnetic-dipole, they could possibly be explained by finite-temperature effects.<sup>31</sup> These components, not allowed by the symmetry, seem therefore unnecessary at our current state of knowledge.

Those components which are allowed by symmetry, however, are most probably important to understand refined experiments, such as the high-field plateau phases<sup>32,33</sup> where typical condensation energies are much smaller than the isotropic couplings. For instance, the  $1/8$  plateau width is of order of 1 Kelvin and it is questionable whether Heisenberg models alone capture the essential superstructure of that phase. This provides fur-

ther motivation to quantify to what extent the isotropic model applies to  $\text{SrCu}_2(\text{BO}_3)_2$ , and in what circumstances the anisotropic couplings can be safely neglected.

The paper is organized as follows. In section II, we give the dispersion of the first-triplet excitations for the Heisenberg-Shastry-Sutherland model. In section IIIA, we present the anisotropic model for  $\text{SrCu}_2(\text{BO}_3)_2$  with Dzyaloshinskii-Moriya interactions, and in IIIB) map it onto a simpler model. We then calculate the magnon dispersion both perturbatively (section IV), and by exact diagonalization of finite lattices (section V). We discuss experimental results in section VI and extract the couplings that previously could not be quantified by comparing exact spectra with experimental results.

## II. DISPERSION OF THE LOWEST TRIPLET EXCITATION OF THE SHASTRY-SUTHERLAND MODEL

We first consider the Shastry-Sutherland model<sup>3</sup> (with no Dzyaloshinskii-Moriya interaction), as originally used<sup>4</sup> to describe  $\text{SrCu}_2(\text{BO}_3)_2$ :

$$H = \sum_{nn} J S_i \cdot S_j + \sum_{nnn} J^0 S_i \cdot S_j \quad (1)$$

where  $nn$  stands for nearest neighbors (intra-dimer) and  $nnn$  for next nearest neighbors (inter-dimer). The lattice of couplings is as shown in Figure 2: nearest neighbour couplings are on the diagonals in every second square of the lattice of next-nearest-neighbour couplings (in the real lattice the angles are such that the diagonals are shorter). The strengths of the Heisenberg couplings are  $J = 85$  Kelvin for the nearest-neighbor coupling, and  $J^0 = 54$  for the next-nearest-neighbor coupling, as determined<sup>4</sup> from susceptibility measurements. An interplane coupling is present, but it is small ( $J^0 = 8$  K) and frustrated.<sup>4</sup> We therefore restrict ourselves to a two-dimensional version of the model and neglect  $J^0$ . The ratio  $J^0=J=0.62=0.63$  was confirmed to be consistent with the ratio of the first Ramann-active singlet energy to the first triplet energy,<sup>9</sup> a measure independent of the magnetic susceptibility.

We calculate a few low-lying states of the Shastry-Sutherland model [Hamiltonian (1)] on a 32-site cluster using exact diagonalization. This cluster is particularly attractive compared to smaller ones not only because it has smaller finite size effects, but also because it allows access to the important symmetry points ( $\pi=2$ ;  $\pi=2$ ), ( $\pi$ ;  $\pi$ ) and ( $\pi$ ;  $0$ ) [34]. The results are given in Fig. 1 for  $J^0=J=0.62$ .

The gap between the ground state and the triplet state is  $0.442J$  for the 32-site cluster and essentially independent of the system size as shown in table I. Yet the absence of finite-size effects on the gap does not mean that all energies have reached their thermodynamic limit. In fact the dispersion of the 16-site cluster is much flatter than that of the 20 or 32-site clusters. It has appeared

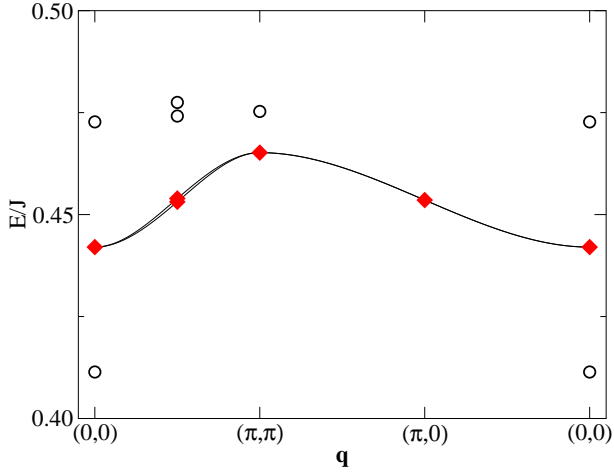


FIG. 1: (color online). Dispersion relation of the first triplet excitation of the Heisenberg Shastry-Sutherland model (diamonds), as calculated by exact numerical diagonalization on a 32-site cluster, for  $J^0=J=0.62$ . The vertical axis shows the excitation energy of those states with respect to the ground state. The degeneracy of the two triplets at  $(\pi, \pi)$  is slightly lifted, reflecting the two dimers per unit cell. Singlet states nearby are shown as open circles.

before (but for the simple square lattice) that the 16-site cluster can be quite special compared with larger clusters.<sup>35</sup> Comparison of the bandwidths of the 20-site and 32-site clusters is also difficult because the reciprocal points are not identical. In particular the bandwidth of the 20-site cluster is inherently smaller because of the absence of the  $(\pi, \pi)$  reciprocal point: the only non-zero point in reciprocal space is at  $(\frac{2}{5}, \frac{4}{5})$ . Therefore while finite-size effects are definitely smaller than the table might suggest it is not possible to quantify them at present. In absolute values, the bandwidth of the 32-site cluster remains very small,  $0.023J$ , i.e. about 2 K/Elvin. We note that it is smaller than that of the perturbative calculation,<sup>25,26</sup> although this may be explained in part by finite-size effects, but is also qualitatively different in shape. Consistent with the fact that there are two dimers per unit-cell, we have in fact not one but two triplet states which are degenerate at high symmetry points of reciprocal space. The degeneracies are slightly lifted for intermediate  $q$ -values. This splitting was shown to occur at higher order,  $(J^0=J)^{10}$  in perturbation theory.<sup>26</sup> The gap and especially the dispersion relation are in fact much more affected by the smaller anisotropic interactions, as will be shown in the next section.

### III. MODEL AND EXACT MAPPING

#### A. The general anisotropic model

We now consider a model with Dzyaloshinskii-Moriya interactions, based on the symmetries of the low tem-

| cluster size | spin gap   | bandwidth |
|--------------|------------|-----------|
| 16           | 0.460 125J | 0.003 15J |
| 20           | 0.451 441J | 0.015 98J |
| 32           | 0.442 026J | 0.023 16J |

TABLE I: The spin gap and bandwidth of the first triplet excitation in the Shastry-Sutherland model for different cluster sizes. The bandwidth of the 20-site cluster cannot be directly compared with the others because of the absence of the  $(\pi, \pi)$  reciprocal point.

perature phase.<sup>18,19,20</sup> The model contains isotropic couplings,<sup>4</sup> and both inter-dimer<sup>9,12</sup> and intra-dimer Dzyaloshinskii-Moriya interactions.<sup>14</sup> It reads:

$$H = \sum_{ij} [JS_i \cdot S_j + D_{ij} \cdot (S_i \times S_j)] + \sum_{nnn} [J^0 S_i \cdot S_j + D_{ij}^0 \cdot (S_i \times S_j)] \quad (2)$$

where  $nn$  stands for nearest neighbors (intra-dimer) and  $nnn$  for next-nearest neighbors (inter-dimer). The different components of the vectors  $D_{ij}$  and  $D_{ij}^0$  are given in Fig. 2. They are obtained by using transformation

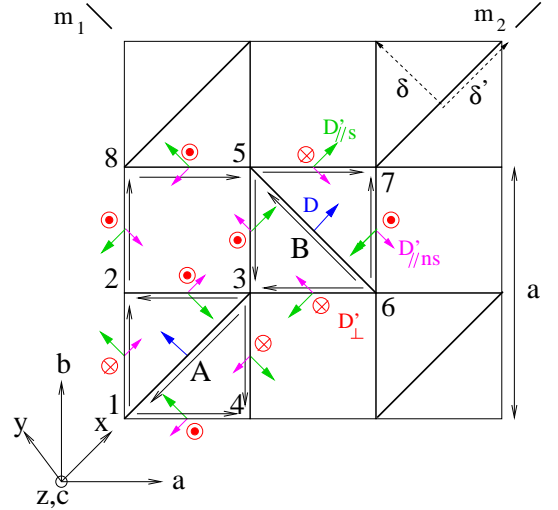


FIG. 2: (color online). Shastry-Sutherland lattice with Dzyaloshinskii-Moriya interactions allowed by the symmetries of  $\text{SrCu}_2(\text{BO}_3)_2$ . Colored (short gray) arrows are the components of the Dzyaloshinskii-Moriya vectors for each bond (long arrows show the prescription for the order of the operators, a black arrow from  $i$  to  $j$  indicates that we should take  $D_{ij} \cdot (S_i \times S_j)$  with the given  $D_{ij}$ ).  $m_1$  and  $m_2$  are mirror planes, but the  $(ab)$  plane is not a mirror plane in the low-temperature phase. This allows for all in-plane components of  $D$ .

properties of pseudo-vectors and the symmetries of the crystal structure.<sup>11</sup> For instance, when a bond connecting two spins belongs to a mirror plane, the Dzyaloshinskii-Moriya vector must be perpendicular to it. In the high

temperature phase ( $T > 400$  K),<sup>19</sup> the (ab) plane is a mirror plane and the allowed components (only the inter-dimer ones) must therefore be parallel to the crystallographic c-axis. This is the  $D_{ij}^0 = D_z^0 \hat{e}_z$  ( $\hat{e}_z$  is the unit vector along  $z = c$ ) we considered before. In the low temperature phase, the (ab) plane is slightly buckled, and some other in-plane components are allowed, but are expected to be smaller.<sup>12</sup> The remaining  $m_1, m_2$  mirror planes allow us to determine the complete pattern of Dzyaloshinskii-Moriya vectors. In-plane components of  $D_{ij}^0$  can be decomposed into staggered  $D_{k,ns}^0$  and non-staggered  $D_{k,ms}^0$  orthogonal components. We obtain

$$D_{ij}^0 = D_{k,ns}^0 \hat{e}_{s;ij} + D_{k,ms}^0 \hat{e}_{ns;ij} + D_z^0 \hat{e}_z \quad (3)$$

where the unit vectors are, respectively,  $\hat{e}_{s;ij} = \hat{e}_y$  and  $\hat{e}_{ns;ij} = \hat{e}_x$  (for dimers A) or  $\hat{e}_{s;ij} = \hat{e}_x$  and  $\hat{e}_{ns;ij} = \hat{e}_y$  (dimers B) (Fig. 2). The intra-dimer vector  $D_{ij}$  has only in-plane components,

$$D_{ij} = D \hat{e}_{ij} \quad (4)$$

with the unit-vector  $\hat{e}_{ij} = \hat{e}_y$  (dimers A) or  $\hat{e}_{ij} = \hat{e}_x$  (dimers B). Note that because the interaction is a vector product of spins, we have to be careful with the order of the operators in the definitions. The order is defined in Fig. 2 for each bond by the black arrows. For instance, for the bond 1 → 2, we define  $D_{12}^0 = D_{k,ns}^0 \hat{e}_y + D_{k,ms}^0 \hat{e}_x + D_z^0 \hat{e}_z$ . The strengths of three of these four couplings,  $D$ ,  $D_{k,ns}^0$ ,  $D_{k,ms}^0$ , are unknown. In the next paragraph, we show how to simplify the Hamiltonian (2) such as to eliminate two of these couplings. Eventually only one parameter remains to be determined and we will determine it with the help of the magnon dispersion at finite wave-vector.

### B. Mapping

We map the Hamiltonian (2) onto a simpler Hamiltonian with no intra-dimer and no uniform Dzyaloshinskii-Moriya interactions, by means of rotations<sup>21</sup> of spin operators. Contrary to previous situations where this approach has been applied,<sup>21,36</sup> it turns out here that we cannot eliminate all components, because of the frustration of the lattice but we can nonetheless simplify the model. For this, we perform two sorts of rotations. First, we rotate the two spin operators of the dimers in opposite directions, and apply the same operation to all unit cells. Second, we rotate the spin operators from dimer to dimer by applying the same operation to the two spin operators of the same dimer. The first transformation uses local rotations (the same for all unit-cells) for the two spins  $i$  and  $j$  of the dimer  $ij$ , that are defined by:

$$S_i^0 = R(\pi/2; \hat{e}_{ij}) S_i \quad (5)$$

$$= (1 - \cos \frac{\pi}{2}) [\hat{e}_{ij} \cdot S_i] \hat{e}_{ij} + \cos \frac{\pi}{2} S_i - \sin \frac{\pi}{2} S_i \times \hat{e}_{ij} \quad (6)$$

with  $\tan \theta = D/J$ ,<sup>21</sup> where  $D$  and  $\hat{e}_{ij}$  are defined by (4). The second spin  $j$  of the same dimer is rotated in the opposite sense (←). For the second dimer of the unit-cell, the spins are rotated similarly, about an axis that is perpendicular to that, according to the local  $D_{ij}$  (see Fig. 2).

We now restrict consideration to terms that are linear in the Dzyaloshinskii-Moriya coupling strength in the transformation (6), because we are looking for linear effects in the dispersion of excitations. In fact the transformation (6) does produce some anisotropic exchange of order  $D^2/J$ ,<sup>21</sup> which we neglect because (i) we have not taken into account real anisotropic couplings which occur at the same order of magnitude, and more importantly, (ii) the spectrum is fully dominated by effects that are linear in  $D$ , as we shall show.

In terms of the primed spins, the Hamiltonian (2) is mapped onto (up to terms of order  $D^2/J$ ):

$$H = \sum_{nn} J S_i^0 \cdot S_j^0 + \sum_{nnn} J^0 S_i^0 \cdot S_j^0 + D_{ij}^0 (S_i^0 \cdot S_j^0) \quad (7)$$

where the  $D_{ij}^0$  are now modified: the staggered c-component is unchanged, whereas the strengths of the in-plane components (either staggered or uniform) are modified according to

$$D_{k,ms}^0 \rightarrow D_{k,ms}^0 + \frac{J^0}{2J} D \quad (8)$$

$$D_{k,ns}^0 \rightarrow D_{k,ns}^0 + \frac{J^0}{2J} D \quad (9)$$

$$D_z^0 \rightarrow D_z^0 \quad (10)$$

This is an exact transformation that is valid at all order in  $J^0/J$ . As a second step, we now proceed to eliminate the non-staggered component of  $D_{ij}^0$ , which is defined by its strength  $D_{k,ms}^0$  (eq. (8)) and a vector direction either along  $x$  or  $y$  (see Fig. 2). This is made possible because the  $D_{k,ms}^0$  sum up to zero along any closed loop of the lattice. When going around closed loops, the rotation angles are fixed by the Dzyaloshinskii-Moriya strength and sign; therefore there is a compatibility condition for the last spin.<sup>37</sup> Consider for instance the closed loop (2 → 8 → 5 → 3 → 2) in Fig. 2, the sum of the  $D_{k,ms}^0$  is zero along this loop. Note, however, that the sum of the  $D_z^0$  does not vanish, nor does the sum of the  $D_{k,ns}^0$  along (5 → 7 → 6 → 5), for instance, so these cannot be eliminated. We now rotate the operators accordingly, and restrict to the first-order terms in  $D_{k,ms}^0$ :

$$S_i = R(\theta_i; \hat{e}_y) R(\theta_i; \hat{e}_x) S_i^0 \quad (11)$$

In this expression,  $\theta_i = (D_{k,ms}^0/J^0) R_i \cdot \hat{e}_x$ , and  $\theta_i = (D_{k,ms}^0/J^0) R_i \cdot \hat{e}_y$ , where  $\hat{e}_{x/y}$  are unit vectors along the  $x$  and  $y$  directions.  $R_i$  is the position of the dimer to which the spin  $i$  belongs, in units of the inter-dimer spacing. The two spins of the same dimer are rotated in the same way, so as not to generate other intra-dimer

Dzyaloshinskii-Moriya interactions. The final Hamiltonian becomes:

$$H = \sum_{nn} J S_i \cdot S_j + \sum_{nnn} J^0 S_i \cdot S_j + \vec{D}_{ij} \cdot (S_i - S_j) \quad (12)$$

$$\vec{D}_{ij} = \vec{D}_k \hat{e}_{s,ij} + \vec{D}_? \hat{e}_z \quad (13)$$

$$\vec{D}_k = D_{k;s}^0 + \frac{J^0}{2J} \vec{D} \quad \vec{D}_? = D_?^0 \quad (14)$$

where  $\hat{e}_{s,ij}$  is the unit-vector along the inter-dimer staggered Dzyaloshinskii-Moriya vector, defined in Fig. 2. The transformed model (12) is simpler and can be used instead of the original Hamiltonian (2), as far as energies are concerned. The remaining Dzyaloshinskii-Moriya components (13) which we call irreducible cannot be eliminated by rotations. Geometrically this is because they do not sum to zero when turning around closed loops of the Shastry-Sutherland lattice. As a consequence, linear effects are present in the spectrum.

We shall proceed with the Hamiltonian (12) since the two Hamiltonians have exactly the same energy spectrum up to terms of order  $D^2=J$ ,  $D_{k;n s}^0=J$ . Note that this is valid only at zero magnetic field: at finite fields along  $z$ , for instance, the first transformation creates a staggered transverse field<sup>36</sup> (which must already be present according to the local environment surrounding the copper ions<sup>4</sup>) and the second transformation creates rotating fields.

#### IV. PERTURBATIVE CALCULATION OF THE EXCITATION SPECTRUM

We calculate the magnon dispersion and dynamical structure factor of model (12), by first-order perturbation theory in the Dzyaloshinskii-Moriya couplings and  $J^0=J$ .<sup>9,12</sup> Since the latter is not small for  $\text{SrCu}_2(\text{BO}_3)_2$  ( $J^0=J = 0.62-0.63$ ), we will supplement this approximation with exact numerical results in section V but perturbation theory already gives some qualitative insights into the problem.

We start with the exact dimer ground state, which is a product of singlets on each dimer. We consider the following one-particle excited states, which consist of promoting a dimer into a triplet state with  $S^z = 0; \pm 1$  quantum number. They are the eigenstates for zero  $J^0$  and  $\vec{D}$ , and we use first-order perturbation theory in  $J^0=J$ ,  $\vec{D}_k$  and  $\vec{D}_?$ . Because there are two dimers per unit-cell, there are two such triplet states depending on which dimer A or B is in the triplet state. When  $\vec{D}_?$  is added, the total rotation invariance is broken but  $S^z$  is still a good quantum number thanks to the rotation about  $c$ . In this case, the eigenstates within this subspace of states are given by:<sup>9</sup>

$$|\mathcal{J}^z; q; i\rangle = \frac{1}{\sqrt{2}} (|\mathcal{J}^z; q; A i\rangle - i |\mathcal{J}^z; q; B i\rangle) \quad (15)$$

with  $S^z = 0; \pm 1$  the  $z$  component of the total spin of a dimer, and  $|\mathcal{J}^z; q; A i\rangle$  is the Fourier transform of the

triplet state on the dimer A of unit-cell  $i$ ,  $|\mathcal{J}^z; i; A i\rangle$ . Now in addition we consider the effect of inter-dimer staggered components of the Dzyaloshinskii-Moriya vectors i.e. model (12).  $\vec{D}_k$  breaks the rotation invariance about  $c$  and therefore mixes various  $S^z$  components of (15). The Hamiltonian within the subspace of (15) splits into two blocks. The first block for  $(j+1; q; +i; j; q; -i; j+1; q; +i)$  reads

$$\begin{pmatrix} 0 & J + \vec{D}_? \cdot \vec{f}(q) & i\vec{D}_k \cdot \vec{g}(q) & 0 \\ i\vec{D}_k \cdot \vec{g}(q) & J & i\vec{D}_k \cdot \vec{g}(q) & 0 \\ 0 & i\vec{D}_k \cdot \vec{g}(q) & J & \vec{D}_? \cdot \vec{f}(q) \end{pmatrix} \begin{pmatrix} B \\ C \\ A \\ D \end{pmatrix} \quad (16)$$

where we have  $\vec{f}(q) = 2 \cos(q_x/2) \cos(q_y/2)$  and  $\vec{g}(q) = (\sin[(q_x + q_y)/2] + i \sin[(q_x - q_y)/2]) \hat{e}_z$ ,  $q = (q_x; q_y)$ . The lattice spacing is taken such that  $a = 1$ . The second block for the three other states, is identical up to the change  $(\vec{D}_k; \vec{D}_?) \rightarrow (-\vec{D}_k; \vec{D}_?)$ . The six resulting triplet states are denoted by  $|\mathcal{J}_q^m i\rangle$  and have energies (twice degenerate because of identical blocks):

$$E_{\pm}(q) = J \pm \sqrt{(\vec{D}_? \cdot \vec{f}(q))^2 + 2(\vec{D}_k \cdot \vec{g}(q))^2} \quad J \pm \frac{q}{2} \quad (17)$$

The dispersion relations of "triplet" states (17) are given in Fig. 3. They are valid only at first-order in  $J^0=J$  and higher-order corrections are not included here. We shall see below how the overall shape and degeneracies are modified when one goes beyond perturbation theory. For the moment, this defines two splittings at  $q = (0;0)$  and  $q = (\pi;0)$  that are given by:

$$E_{\pm}(0;0) = 4\vec{D}_? \cdot \vec{f} = 4D_?^0 \quad (18)$$

$$E_{\pm}(\pi;0) = \frac{J^0}{2} \pm 2\vec{D}_k \cdot \vec{g} = \frac{J^0}{2} \pm D_{k;s}^0 + \frac{J^0}{2J} D \quad (19)$$

where the right-hand sides give the expressions of the splittings in terms of the original couplings of Fig. 2, according to the transformations (9) and (10). It is interesting to note that measuring these splittings at different wave-vectors allows, in principle, separation of the two couplings. This is because of the different staggering patterns of the Dzyaloshinskii-Moriya vectors in space, which is itself a consequence of the crystal symmetry.

In order to compare with neutron inelastic scattering at finite wave-vectors, we have computed the neutron cross-section, given by<sup>38</sup>

$$\frac{d^2}{d\Omega dE} \propto \sum_m |S_q^m(q)|^2 |\vec{E}^m(q)|^2 \quad (20)$$

$$S_q^m(q) = \sum_i \frac{q_i q_j}{q^2} \langle 0 | S_q^m | \mathcal{J}_q^m i \rangle \langle \mathcal{J}_q^m i | S_{-q}^m | 0 \rangle \quad (21)$$

Note that  $S_q$  is, strictly speaking, the real spin operator, not that obtained after the transformations are performed,  $S_q^*$ . We can in fact replace  $S_q$  by  $S_q^*$  because it

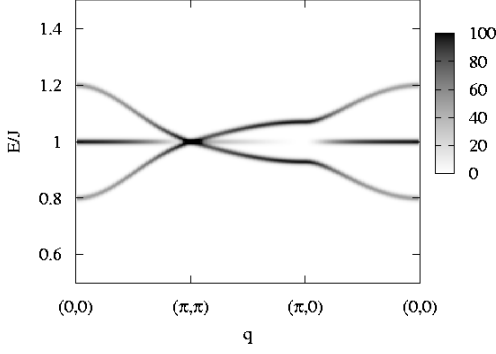


FIG. 3: ( $J^0=J \neq 0$ ) Dispersion relation and dynamic structure factor (grey scale) of the first triplet excitations in the limit of small  $J^0=J$ . Note the overall dimer form factor  $M_q$  is not included in the picture. For  $(\pi; 0)$ , the middle mode has no intensity. For the clarity of the picture,  $D_\pi = 0.1J$ , and  $D_k = 0.05J$  were used.

implies small intensity corrections, of order  $D=J$ , which we shall discuss later in the paper. The cross-section involves calculating all matrix elements. Some do not contribute for special directions of the reciprocal vector, such as for those along the reciprocal line  $q = (q; 0)$  ( $q$  parallel to  $a$  gives geometrical factors  $q_a^2 = q^2 = 1$ ,  $q_b^2 = q_c^2 = 0$ ), and only  $H_q^m \beta_q^b \beta_i$  and  $H_q^m \beta_q^c \beta_i$  contribute. For  $q = (q; q)$  and  $q = (q; 0)$ , the intensities have the form

$$S^0(q) = \frac{2D_\pi f(q)}{q} M_q + \frac{2D_k g(q)}{q} M_q + \frac{1}{2} + \frac{2D_k h(q)}{q} M_q + \dots$$

where  $M_q = \sin^2 q_a + \sin^2 q_b$  is the form factor of the unit-cell,  $2$  and  $2^0$  being the vectors along the dimer  $A$  and  $B$  (Fig. 2). The dots represent corrections of order  $O(D; D_{k,n.s.})$ , whereas the intensities are  $O(1)$ . We will come back to this when discussing the effect of  $D$  and  $D_{k,n.s.}$ . For  $q = (\pi; q)$ , the  $q$  dependence comes only from the geometrical factor:

$$S^0((\pi; q)) = \frac{q^2}{2 + q^2} M_q + \dots$$

$$S^1((\pi; q)) = \frac{1}{2} \frac{2 + q^2}{2 + q^2} M_q + \dots$$

The intensities (eqs. (22)–(25)) are represented in grey scale in Fig. 3 ( $M_q$  is not included). We see, in particular,

that the intensity of the middle mode at  $(\pi; q=0)$  is zero. This is consistent with the presence of only two modes in neutron scattering experiments at that wave-vector,<sup>12,13</sup> and allows us to identify these modes as the lower and upper modes (as will be confirmed by their energies later as well).

## V. EXACT NUMERICAL DIAGONALIZATION

We calculate a few low lying states of the Hamiltonian (12) on the 32-site cluster using exact diagonalization. Note that the  $D_k$  term in (12) breaks spin rotational symmetry and the dimension of the Hilbert space now becomes  $5 \cdot 10^8$ , as compared to  $7 \cdot 10^7$  for the 32-site cluster of the Shastry-Sutherland model. Results are shown in Fig. 4. The parameters are  $J^0=J = 0.62$ ,  $D_\pi = 0.02J$  and  $D_k = 0.005J$ . It is to be compared with Fig. 1 which corresponds to  $D_\pi = D_k = 0$ . Since  $S^z$  is no longer a good quantum number, degeneracies in those triplet states in Fig. 1 are lifted. Nevertheless, they can still be grouped together according to whether their energies increase, decrease or remain unchanged in the presence of a weak magnetic field along the  $c$  direction, which correspond to  $S^z = +1$ ,  $-1$ , and  $0$  respectively in the limit  $D_k \rightarrow 0$ . In Fig. 4 states belonging to the same group at different  $q$  are joined together by a line. Note that the middle state, which corresponds to the  $S^z = 0$  and indicated by diamonds, is almost unchanged with respect to Fig. 1. But the others acquire a larger dispersion that in any case remains small compared to the gap.

Next we study in detail the effects of  $D_\pi$  and  $D_k$  on

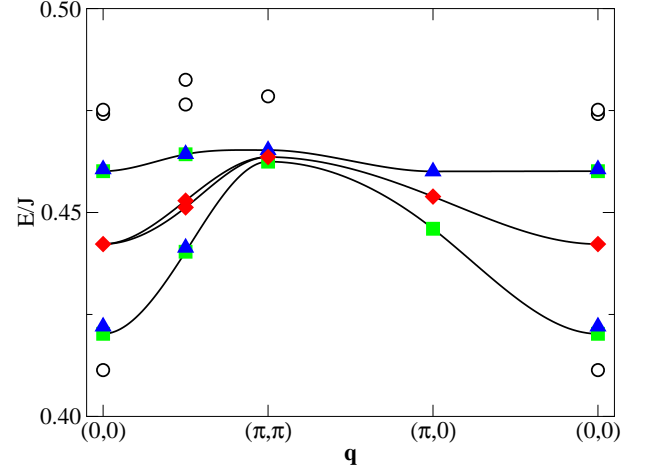


FIG. 4: (color online) Same as Fig. 1 but for the Hamiltonian (12) with  $J^0=J = 0.62$ ,  $D_\pi = 0.02J$  and  $D_k = 0.005J$ . Lines are guides to the eye and join together states which would correspond to  $S^z = +1$  (triangles),  $-1$  (squares), and  $0$  (diamonds) in the limit  $D_k \rightarrow 0$ . Note that some of them are indistinguishable for the upper mode.

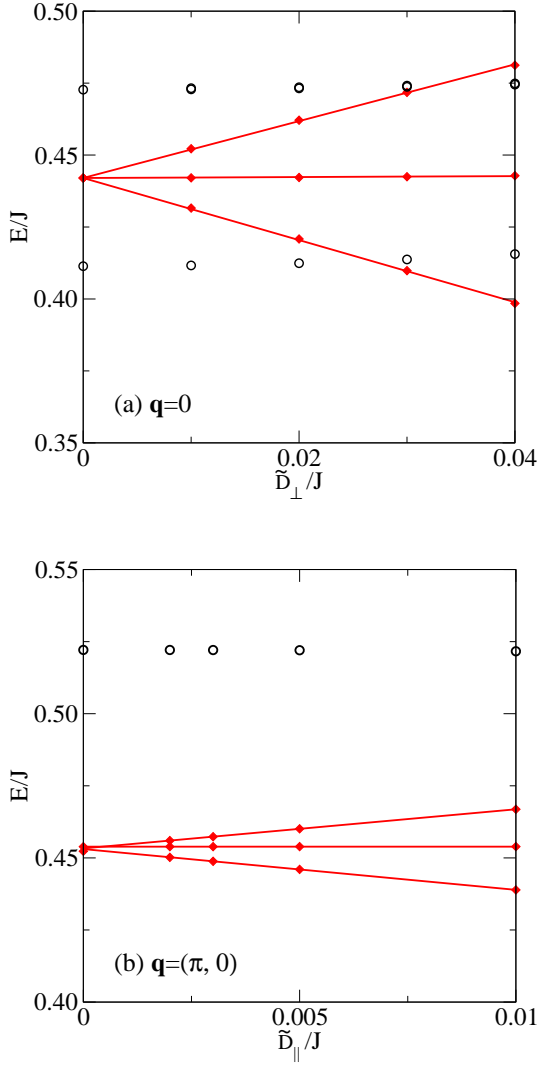


FIG. 5: (a) Effect of  $\tilde{D}_\perp$  on the  $q = 0$  triplet (diamonds) and singlet energies (open circles) when  $\tilde{D}_k = 0$ , and (b) effect of  $\tilde{D}_k$  on the  $q = (\pi, 0)$  states when  $\tilde{D}_\perp = 0.02J$ . Numbers are calculated using exact diagonalization on the 32-site cluster. Lines are linear fittings to triplet energies.

the splitting of the first triplet state. Fig. 5(a) shows the splitting in the  $q = 0$  "triplet" state at various  $\tilde{D}_\perp$  and  $\tilde{D}_k = 0$ . We found that a small  $\tilde{D}_k$  ( $0.005J$ ) has no noticeable effect on the splitting of the  $q = 0$  states. Therefore Fig. 5(a) can be regarded as showing the effect of  $\tilde{D}_\perp$  on the splitting of those states. Fig. 5(b) shows the splitting of the first triplet state at  $q = (\pi, 0)$  at  $\tilde{D}_\perp = 0.02J$  and various  $\tilde{D}_k$ . It is clear that the effect of  $\tilde{D}_k$  is to modify the dispersion around the reciprocal point  $(\pi, 0)$ . At  $(\pi, 0)$ , Fig. 5(b) shows that the energies change linearly as function of the coupling, except at very small  $\tilde{D}_k$ . In this region, a very small gap already exists, and is given by  $\tilde{D}_\perp$  ( $J^0=J$ ) (where  $> 1$ ). In absolute values we have found a gap of  $1.6 \times 10^{-3}J$  (for  $\tilde{D}_\perp = 0.02J$ ). The tiny gap is amplified by  $\tilde{D}_k$  and the effect is perturbative in

the strength of the Dzyaloshinskii-Moriya interactions. Note that the slopes, however, are a function of  $J^0=J$  and are non-perturbative in this coupling. First, for values of  $J^0=J$  close to the critical point, the separation of the components as in (18) and (19) is no longer exactly true, but the effect of  $\tilde{D}_k$  at  $q = 0$  remains small (and conversely) in the regime of interest. Second, the prefactors of the splittings between the upper and lower modes are modified compared to the perturbative results. From linear fittings as shown in Fig. 5, the splitting at  $q = 0$  is found to be  $2.08\tilde{D}_\perp$  instead of  $4\tilde{D}_\perp$  in (18). This compares very favorably with a previous calculation using the 20-site cluster,<sup>9</sup> thus showing that size effects are small. Similarly at  $q = (\pi, 0)$  the splitting is  $2.80\tilde{D}_k$  instead of  $2\tilde{D}_k$  in (19). Note that the renormalization at  $q = (\pi, 0)$  is in fact very small compared to that at  $q = 0$ , and solves the puzzle previously noticed,<sup>13</sup> as we shall explain below.

The spectra show other minor features: at  $q = 0$ , for instance, the lowest state is split into two (Fig. 4). This is to be expected when there are several anisotropy axes and no Kramers degeneracy in a system with an even number of spins per unit-cell. We can simply understand these additional splittings by perturbation theory: couplings with higher energy states open gaps which scale as  $\tilde{D}_k^2$  (which we verified by exact diagonalization). The exact calculation shows other  $\tilde{D}_k^2$  effects. We cannot make quantitative comparison of effects at this order to real experiments because anisotropic super-exchange is also present at order  $\tilde{D}_k^2$  and are neglected in the present work.  $\tilde{D}_k^2$  effects may perhaps be accessible to ESR at  $q = 0$ , but it might be difficult to disentangle the second-order effects of Dzyaloshinskii-Moriya from that of real asymmetric couplings.

## VI. EXTRACTING THE COUPLINGS FROM EXPERIMENTS

Triplet states. We now use these results to extract the anisotropic couplings from neutron inelastic scattering experiments. At  $q = 0$ , we have seen that the energy is unchanged between the 20-site cluster<sup>9</sup> and the present 32-site cluster, so the estimation of  $D_\perp^0 = 0.18$  meV is unmodified. Regarding the intensity at  $q = 0$ , earlier perturbative calculation<sup>9</sup> compares well with exact numerical diagonalization on a 20-site cluster,<sup>39</sup> so we have not carried out intensity calculations on the 32-site problem, but will rely on perturbative results. At  $q = (\pi, 0)$ , we have seen indeed that the intensity of the middle mode is zero (section IV). This is consistent with the observation of vanishing intensity for the middle mode in neutron scattering.<sup>12,13</sup> The splitting seen at  $q = (\pi, 0)$  can therefore be interpreted as the gap between the lower and upper state. As we have seen, the splitting at  $q = (\pi, 0)$  is given by  $\tilde{D}_k f$  ( $J^0=J$ ), with  $f(0) = 2\sqrt{2}$  and  $f(0.62) = 2.80$  (which is in fact within 1% of the perturbative result).



This allows to extract  $D_k^0 = 0.07$  meV, taking a splitting  $(\pi; 0) = 0.2$  meV<sup>12,13</sup>. This is the value we extracted before relying on the perturbative expression.<sup>12</sup> We have here calculated the renormalization coefficient at  $(\pi; 0)$ , and shown that that coefficient is quite different from that at  $(0; 0)$ ; therefore applying the same renormalization to both splittings<sup>13</sup> leads to an artificially large in-plane Dzyaloshinskii-Moriya coupling. This explains why the ratio appeared so large previously. In fact, the correct ratio is  $D_k^0 = D_{\pi}^0 = 0.4$  with  $D_{\pi}^0 = 0.18$  meV. We recall that  $D_k^0$  is a linear combination of two interactions (see below), and as such may explain why it is larger than expected on the basis of the small buckling of the crystal structure. We therefore conclude that from the splittings at  $q = (0; 0)$  and  $q = (\pi; 0)$ , we constrain the couplings:

$$D_{\pi}^0 = 0.18 \text{ meV} \quad (26)$$

$$D_{k;S}^0 + \frac{J^0}{2J} D = 0.07 \text{ meV} \quad (27)$$

These values also explain the dispersion of the excitations as shown in Fig. 6, at least for the additional reciprocal points available in the 32-site cluster (diamonds). Note that the scales of experiment and numerical calculations are slightly shifted. The shift could be eliminated by an optimized choice of  $J^0 = J$  in the range 0.62-0.63, consistent with previous estimates.

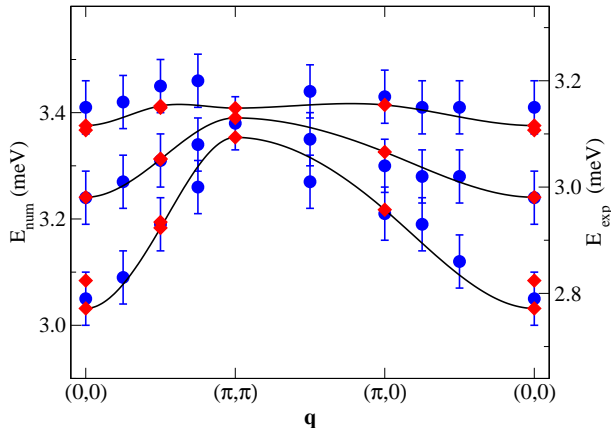


FIG. 6: (color online). Magnon dispersion : exact diagonalization with Dzyaloshinskii-Moriya interactions (diamonds) and experimental data from Ref. [12] (circles). Lines are guides to the eyes. Parameters are  $D_{\pi}^0 = 0.18$  meV, and  $D_k^0 = 0.07$  meV.  $J^0 = J$  was kept equal to 0.62. This is responsible for the shift in the overall scale of the calculated energies.

How could we, at least in principle, determine individually  $D$ ,  $D_{k;S}^0$  and  $D_{k;n;S}^0$ ? As we have shown, the effect of Dzyaloshinskii-Moriya on the spectrum is large only for the two effective components that could not be eliminated by our transformations. To determine the other components, the effect of an external magnetic field

may provide more constraints. However, staggered gyromagnetic tensors come into play, that are also unknown. Alternatively, we can use neutron scattering intensities. First, we calculate the correction to the expressions of the intensities (eq. (22) or (24)) at  $q = (\pi; 0)$ , coming from the intra-dimer Dzyaloshinskii-Moriya interaction,  $D$ . Indeed the spin operators  $S_q$  have a linear correction in  $D$  (see eq. (6)) that we have neglected so far. The intensity at  $q = (\pi; 0)$  (that was zero before) acquires a term proportional to  $(D = J)^2 : S^0((\pi; 0)) = \frac{D^2}{8J^2} N_q$  where  $N_q = \cos^2 q_x + \cos^2 q_y$ . So in principle it is possible to extract  $D$  from measuring the ratio of intensities at  $q = (\pi; 0)$ ,  $\frac{S^0((\pi; 0))}{S^0((0; 0))} = \frac{D^2}{8J^2} \tan^2 \frac{\pi}{6} = \frac{1}{2}$ . This ratio is very small  $0.02(D = J)^2$ , and it therefore seems difficult to extract this coupling independently. Second, we consider the effect on the intensities of the non-staggered components  $D_{k;n;S}^0 + J^0 D = 2J$ , that we had eliminated by the second rotation. Since the rotation is performed using a constant angle when going from dimer to dimer, the spin operators  $S_q$  contains operators that are shifted in  $q$  space,  $S_{q+k_0}$ , where  $k_0$  is determined by the coupling  $D_{k;n;S}^0 + J^0 D = 2J$ . A consequence is that "ghosts" of the original magnon dispersion (as given in Fig. 4) shifted by  $k_0$  must appear in the spectrum. Of course because the shift is small, of order  $\pi/6$ , and the dispersion is of the same order, the energies are changed by  $\pi^2$ . The effect will be difficult to detect by neutron scattering using constant wave-vector scans, but could appear in constant energy scans. This is reminiscent of magnon dispersions in well ordered systems, such as  $\text{Ba}_2\text{CuGe}_2\text{O}_7$ , where the Dzyaloshinskii-Moriya interaction and the helical magnetic structure give rise to three branches in the excitation spectrum.<sup>40</sup>

**Singlet states.** In Figs. 4 and 5, higher and lower singlet states are also given. Since the rotational symmetry is broken, denoting a state as a "singlet" is to be understood as its property for vanishing anisotropies. Singlets are not directly visible by ESR, because the external field is swept at constant wavelengths and only field-dependent states are detected. Nonetheless the bending of the triplet energy levels tend to signal a level anti-crossing with a singlet: experimentally such bendings were observed and thus singlet energies indirectly measured.<sup>43</sup> The measured anti-crossings are at 2.67 meV (compared to the lowest triplet state at 2.81 meV) and 3.56 meV (compared to the higher triplet at 3.16 meV).<sup>43</sup> In Fig. 4 the lowest singlet has an energy which is 95% of the triplet gap, in good agreement with the experimental figure. However the second singlet seems to be higher in energy compared to that of Fig. 4. We know that there are other singlet states at higher energies, and that observed by ESR may be one of them.

**Sign of the coupling.** We remark that although the sign of  $D_{\pi}^0$  is of no consequence on the energy spectrum, it interchanges the "handedness" of the wave functions of the upper and lower states. It therefore has measurable consequences when polarized light interacts with the



triplets.<sup>29</sup> It is interesting to note that the sign of  $D_z^0$  extracted by analyzing<sup>29</sup> far-infrared experiments<sup>8,30</sup> is opposite to that suggested to explain avoided crossing at higher elds.<sup>14,15</sup> The apparent contradiction may be resolved because the avoided crossing is not determined solely by  $D$ , as suggested earlier<sup>14,15,16</sup>, but rather by a combination of  $D_{k,rs}^0 + J^0 D = 2J$ ,  $D_{k,ms}^0 + J^0 D = 2J$  and the staggered elds. Quantitative understanding of the avoided crossing would need determination of each individual coupling.

## VII. CONCLUSIONS

We have considered a model for  $\text{SrCu}_2(\text{BO}_3)_2$  with all the Dzyaloshinskii-Moriya interactions compatible with the crystal structure, i.e. a model with all anisotropic couplings linear in the spin-orbit coupling. We have constructed a simpler anisotropic Hamiltonian (12) with a smaller number of couplings, by appropriate mappings, which has nonetheless exactly the same spectrum up to second-order interactions. The transformation allowed us to separate what we term the "reducible" components of Dzyaloshinskii-Moriya vectors (the non-staggered components  $D_{k,ms}^0$  and part of the intra-dimer interaction  $D$ ) from the "irreducible" (the staggered  $D_z^0$ ,  $D_{k,rs}^0$  with a contribution from the intra-dimer interaction  $D$ ). By definition the latter have effects on the spin excitation spectrum that are linear in the strength of the coupling, whereas the former have second-order effects. The linear effect arises, precisely, because we cannot eliminate these components. Had we been able to eliminate all of them, we should have taken into account anisotropic symmetric exchanges, on an equal footing.<sup>21</sup> In that case, depending on the underlying superexchange processes, one may recover a fully rotationally invariant spectrum (if single-orbital processes are dominant),<sup>21</sup> or not (when multi-orbital processes exist).<sup>41</sup> In any case, the effects would have been at most <sup>2</sup>, and very difficult to extract experimentally because this would be of order of a few eV. In contrast,  $\text{SrCu}_2(\text{BO}_3)_2$  represents a real situation where the bond frustration leads to an energy scale of order hundreds of eV here in the spin excitation spectrum.

We have explained quantitatively the dispersion of the lowest triplet states (Fig. 6) which is dominated by Dzyaloshinskii-Moriya interactions (compare Fig. 1 and 4). First-order perturbation theory was not sufficient to account quantitatively for the dispersion shape (see Fig. 3) but allows us to capture most of the symmetries except for the small additional splittings due to the presence of two dimers per unit cell. Measurements of the dispersion under high-pressure<sup>42</sup> should in fact be carefully interpreted: the evolution of the bandwidth with pressure should primarily reflect the change in the Dzyaloshinskii-Moriya couplings and not the change in the ratio  $J^0=J$  that measure the proximity to the critical point. The

spin gap, where the effect of Dzyaloshinskii-Moriya is secondary, may serve as a more sensitive probe for the proximity to the critical point.

The model (12) whose parameters have been quantitatively determined, may serve as a good starting point to understand other properties of  $\text{SrCu}_2(\text{BO}_3)_2$  at zero eld, such as higher energy bound states. These states, as observed in particular by ESR,<sup>43</sup> Raman scattering,<sup>6,10</sup> far-infrared spectroscopy,<sup>30</sup> and neutron scattering<sup>5,44</sup> have been analyzed so far within the framework of the Shastry-Sutherland model,<sup>45,46,47</sup> but should be affected by Dzyaloshinskii-Moriya interactions. This may explain the splittings observed,<sup>44</sup> and resolve the issue of "localization" versus "delocalization" of these excitations. The large dispersion seen first in ref. [5] and supported by theoretical calculations on the Shastry-Sutherland model was revealed later to be composed of several more localized excitations.<sup>44</sup> This remains to be fully understood and model (12) may help.

We have focused on zero-eld results: finite eld effects are particularly interesting but involve other unknown couplings. If the mappings of section IIIB (transformations (6) and (11)) are made with an external magnetic eld, both an effective staggered eld,<sup>36</sup> and rotating elds appear. As a real staggered eld is already present according to the local symmetry of the copper ions, the net effective elds cannot be known precisely. The level anti-crossing that was found when the spin gap is about to close for a magnetic eld along the  $c$  direction, in particular, cannot be solely due to the intra-dimer interaction, as previously claimed.<sup>14</sup> It has to be seen as a consequence of all these effects: intra and inter-dimer components, and staggered elds.

Interesting developments for doped samples of  $\text{SrCu}_2(\text{BO}_3)_2$  are underway.<sup>48,49</sup> The doped compounds, by breaking translation invariance, may also help to disentangle the different components of the Dzyaloshinskii-Moriya vectors, by studying the induced magnetization of the magnetic ions in the vicinity of the dopant, by NMR for instance.

## Acknowledgments

We are indebted to K. Kakurai for providing with us the experimental data, and for constant encouragement along these lines. We would also like to acknowledge the role of J.-P. Boucher in stimulating our interest in this subject. O.C. and T.Z. would like to thank HKUST for hospitality on several occasions; and O.C. the I.L.L. for hospitality for part of the time. T.Z. and P.W.L. would like to thank the PROCORE program for support which lead to this collaboration. Y.F.C. and P.W.L. are supported by the Hong Kong RGC Grant No. HKUST 6075/02P.

- \* Also at CNRS.
- <sup>1</sup> H. Kageyama, K. Yoshimura, R. Stern, N. V. M ushnikov, K. Onizuka, M. Kato, K. Kosuge, C. P. Slichter, T. Goto, and Y. Ueda, *Phys. Rev. Lett.* **82**, 3168 (1999).
  - <sup>2</sup> S. Miyahara and K. Ueda, *J. Phys.: Condens. Matter* **15**, R327 (2003).
  - <sup>3</sup> B. S. Shastri and B. Sutherland, *Physica* **108B**, 1069 (1981).
  - <sup>4</sup> S. Miyahara and K. Ueda, *Phys. Rev. Lett.* **82**, 3701 (1999); *J. Phys. Soc. Jpn. Suppl. B* **69**, 72 (2000).
  - <sup>5</sup> H. Kageyama, M. Nishi, N. Aso, K. Onizuka, T. Yosihama, K. Nukui, K. Kodama, K. Kakurai, and Y. Ueda, *Phys. Rev. Lett.* **84**, 5876 (2000).
  - <sup>6</sup> P. Lemmens, M. G rove, M. Fischer, G. Guntherodt, V. N. Kotov, H. Kageyama, K. Onizuka, and Y. Ueda, *Phys. Rev. Lett.* **85**, 2605 (2000).
  - <sup>7</sup> H. Nojiri, H. Kageyama, K. Onizuka, Y. Ueda, and M. Motokawa, *J. Phys. Soc. Jpn.* **68**, 2906 (1999).
  - <sup>8</sup> T. Reem, U. Nagel, E. Lippmaa, H. Kageyama, K. Onizuka, and Y. Ueda, *Phys. Rev. B* **61**, 14342 (2000).
  - <sup>9</sup> O. Cepas, K. Kakurai, L.-P. Regnault, T. Ziman, J.-P. Boucher, N. Aso, M. Nishi, H. Kageyama and Y. Ueda, *Phys. Rev. Lett.* **87**, 167205 (2001).
  - <sup>10</sup> A. G ozar, B. S. Dennis, H. Kageyama, and G. Blumberg, *Phys. Rev. B* **72**, 064405 (2005).
  - <sup>11</sup> I. Dzyaloshinskii, *J. Phys. Chem. Solids* **4**, 241 (1958); T. Moriya, *Phys. Rev.* **120**, 91 (1960).
  - <sup>12</sup> K. Kakurai, N. Aso, K. Nukui, M. Nishi, H. Kageyama, Y. Ueda, H. Kadowaki, and O. Cepas, in *Quantum Properties of Low-Dimensional Antiferromagnets*, editors Y. Ajiro and J.-P. Boucher, Kyushu University Press (2002). See also, K. Kakurai, K. Nukui, N. Aso, M. Nishi, H. Kadowaki, H. Kageyama, Y. Ueda, L.-P. Regnault, and O. Cepas, *Progr. Theor. Phys. Suppl.* **159**, 22 (2005).
  - <sup>13</sup> B. D. Gaulin, S. H. Lee, S. Haravifard, J. P. Castellan, A. J. Berlinsky, H. A. Dabkowska, Y. Qiu, and J. R. D. Copley, *Phys. Rev. Lett.* **93**, 267202 (2004).
  - <sup>14</sup> S. Miyahara, F. Mila, K. Kodama, M. Takigawa, M. Horvatic, C. Berthier, H. Kageyama and Y. Ueda, *J. Phys.: Condens. Matter* **14**, S911 (2004).
  - <sup>15</sup> K. Kodama, S. Miyahara, M. Takigawa, M. Horvatic, C. Berthier, F. Mila, H. Kageyama and Y. Ueda, *J. Phys.: Condens. Matter* **17**, L61 (2005).
  - <sup>16</sup> S. Miyahara and F. Mila, *Progr. Theor. Phys.* **159**, 33 (2005).
  - <sup>17</sup> A. Zorko, D. Arcon, H. van Tol, L. C. Brunel, and H. Kageyama, *Phys. Rev. B* **69**, 174420 (2004).
  - <sup>18</sup> R. W. Smith, D. A. Keszler, *J. Solid. State Chem.* **93**, 430 (1991).
  - <sup>19</sup> K. Sparta, G. J. Redhammer, P. Roussel, G. Heger, G. Roth, P. Lemmens, A. Ionescu, M. G rove, G. Guntherodt, F. Hünig, H. Lueken, H. Kageyama, K. Onizuka, and Y. Ueda, *Eur. Phys. J. B* **19**, 507 (2001).
  - <sup>20</sup> K.-Y. Choi, Yu. G. Pashkevich, K. V. Lam onova, H. Kageyama, Y. Ueda, and P. Lemmens, *Phys. Rev. B* **68**, 104418 (2003).
  - <sup>21</sup> T. Kaplan, *Z. Physik B* **49**, 313 (1983); L. Shekhtman, O. Entin-Wohlman, and A. Aharony, *Phys. Rev. Lett.* **69**, 836 (1992).
  - <sup>22</sup> A. Koga and N. Kawakami, *Phys. Rev. Lett.* **84**, 4461 (2000).
  - <sup>23</sup> A. Lauechli, S. Wessel, and M. Sgrist, *Phys. Rev. B* **66**, 014401 (2002).
  - <sup>24</sup> M. Alhajj and J.-P. Malrieu, *Phys. Rev. B* **72**, 094436 (2005).
  - <sup>25</sup> Z. Weihong, C. J. Hamer, and J. Oitmaa, *Phys. Rev. B* **60**, 6608 (1999).
  - <sup>26</sup> C. K netter, E. Muller-Hartmann, and G. S. Uhrig, *J. Phys.: Condens. Matter* **12**, 9069 (2000).
  - <sup>27</sup> G. A. Jorge, R. Stern, M. Jaime, N. Harrison, J. Bonca, S. ElShawish, C. D. Batista, H. A. Dabkowska, and B. D. Gaulin, *Phys. Rev. B* **71**, 092403 (2005).
  - <sup>28</sup> S. ElShawish, J. Bonca, C. D. Batista, and I. Sega, *Phys. Rev. B* **71**, 014413 (2005).
  - <sup>29</sup> O. Cepas and T. Ziman, *Phys. Rev. B* **70**, 024404 (2004).
  - <sup>30</sup> T. Reem, D. Huvonen, U. Nagel, J. Hwang and T. T im usk, H. Kageyama, *Phys. Rev. B* **70**, 144417 (2004).
  - <sup>31</sup> S. Miyashita, A. Ogasahira, *J. Phys. Soc. Japan* **72**, 2350 (2003).
  - <sup>32</sup> K. Onizuka, H. Kageyama, Y. Nanumi, K. K indo, Y. Ueda and T. Goto, *J. Phys. Soc. Jpn.* **69**, 1016 (2000).
  - <sup>33</sup> K. Kodama, M. Takigawa, M. Horvatic, C. Berthier, H. Kageyama, Y. Ueda, S. Miyahara, F. Becca, and F. Mila, *Science* **298**, 395 (2002).
  - <sup>34</sup> See Fig. 1 in P. W. Leung and Y. F. Cheng, *Phys. Rev. B* **69**, 180403 (2004). But note that the meanings of  $J$  and  $J^0$  are interchanged.
  - <sup>35</sup> H. J. Schulz, T. Ziman and D. Poilblanc, *J. de Physique* **6**, 675 (1996).
  - <sup>36</sup> M. Oshikawa and I. A eck, *Phys. Rev. Lett.* **79**, 2883 (1997).
  - <sup>37</sup> O. C. owes M. Oshikawa for this remark. Note that this compatibility condition holds only at first-order in  $D=J$  when the axis of the  $D$ 's are non-collinear (rotations do not commute).
  - <sup>38</sup> see, e.g., G. L. Squires, *Introduction to the theory of thermal neutron scattering*, Cambridge, Cambridge University Press (1978).
  - <sup>39</sup> S. ElShawish, J. Bonca, and I. Sega, *Phys. Rev. B* **72**, 184409 (2005).
  - <sup>40</sup> A. Zheludev, S. Maslov, G. Shirane, I. Tsukada, T. Masuda, K. Uchinokura, I. Zalitznyak, R. Erwin, and L.-P. Regnault, *Phys. Rev. B* **59**, 11432 (1999).
  - <sup>41</sup> W. Koshiba, Y. Ohta, and S. Maekawa, *Phys. Rev. Lett.* **71**, 467 (1993).
  - <sup>42</sup> H. Kageyama, private communication.
  - <sup>43</sup> H. Nojiri, H. Kageyama, Y. Ueda, and M. Motokawa, *J. Phys. Soc. Jpn.* **72**, 3243 (2003).
  - <sup>44</sup> N. Aso, H. Kageyama, K. Nukui, M. Nishi, H. Kadowaki, Y. Ueda, and K. Kakurai, *J. Phys. Soc. Jpn.* **74**, 2189 (2005).
  - <sup>45</sup> Y. Fukumoto, *J. Phys. Soc. Jpn.* **69**, 2755 (2000).
  - <sup>46</sup> K. Totsuka, S. Miyahara, and K. Ueda, *Phys. Rev. Lett.* **86**, 520 (2001).
  - <sup>47</sup> C. K netter and G. S. Uhrig, *Phys. Rev. Lett.* **92**, 027204 (2004).
  - <sup>48</sup> G. T. Liu, J. L. Luo, Y. Q. Guo, S. K. Su, P. Zheng, N. L. Wang, D. Jin, and T. Xiang, *Phys. Rev. B* **73**, 014414 (2006).
  - <sup>49</sup> S. Haravifard, S. R. Dunsiger, S. ElShawish, B. D. Gaulin, H. A. Dabkowska, M. T. F. Telling, T. G. Perring, and J. Bonca, *Phys. Rev. Lett.* **97**, 247206 (2006).